

# **Synthesis of Cu Nanoparticles Incorporated Mesoporous C/SiO<sub>2</sub> for Efficient Tetracycline Degradation**

*Ning Wang<sup>1,2</sup> Yuanyuan Zhao,<sup>1,2</sup> Xuelian Wu,<sup>1,2</sup> Dapeng Li,<sup>3</sup> Ruguang Ma,<sup>1</sup> Zhigang Chen,<sup>1,3</sup> and Zhengying Wu,<sup>\*1,3</sup>*

*<sup>1</sup> Jiangsu Key Laboratory for Environment Functional Materials, School of Materials Science and Engineering, Suzhou University of Science and Technology, Suzhou 215009, China*

*<sup>2</sup> School of Chemistry and Life Science, Suzhou University of Science and Technology, Suzhou 215009, China*

*<sup>3</sup> Jiangsu Collaborative Innovation Center of Technology and Material for Water Treatment, Suzhou University of Science and Technology, Suzhou 215009, China*

*\*Corresponding authors:*

*Zhengying Wu, Tel./fax: +86 512-67374120, Email: [zywu@mail.usts.edu.cn](mailto:zywu@mail.usts.edu.cn);*

<b>Supporting information Texts.....</b>	<b>S4</b>
<b>Text S1.</b> Characterization of the catalysts .....	4
<b>Text S2.</b> Analytical methods for adsorption and catalysis.....	5
<b>Supporting information Table.....</b>	<b>S6</b>
<b>Table S1.</b> N <sub>2</sub> adsorption/desorption results of the C-SiO <sub>2</sub> and Cu/C-SiO <sub>2</sub> . .....	6
<b>Table S2.</b> Reaction rate constants of TC degradation by CuO, Cu, C-SiO <sub>2</sub> , and Cu/C-SiO <sub>2</sub> .....	7
<b>Table S3.</b> The catalytic capacity of different catalysts towards TC. ....	8
<b>Supporting information Figures.....</b>	<b>S9</b>
<b>Figure S1.</b> TG and DSC curves of the template-containing mesoporous SiO <sub>2</sub> sample. ....	9
<b>Figure S2.</b> FTIR spectra of C-SiO <sub>2</sub> , Cu/C-SiO <sub>2</sub> -AS, and Cu/C-SiO <sub>2</sub> . ....	10
<b>Figure S3.</b> Effect of initial TC concentration on the removal of TC (catalyst dosage = 1 g·L <sup>-1</sup> , C <sub>0</sub> = 350–600 mg·L <sup>-1</sup> , H <sub>2</sub> O <sub>2</sub> = 15 mL, T = 20±2 °C): (a) adsorption and total removal efficiencies, (b) fitted rate constant <i>k</i> .....	11
<b>Figure S4.</b> Effect of catalyst dosage on the removal of TC: (a) adsorption and total removal efficiencies, (b) fitted rate constant <i>k</i> (C <sub>0</sub> = 500 mg·L <sup>-1</sup> , H <sub>2</sub> O <sub>2</sub> = 15 mL). .....	12
<b>Figure S5.</b> Effect of H <sub>2</sub> O <sub>2</sub> dosage on the removal of TC: (a) adsorption and total removal efficiencies, (b) fitted rate constant <i>k</i> (catalyst dosage = 1 g·L <sup>-1</sup> , C <sub>0</sub> = 500 mg·L <sup>-1</sup> ).....	13
<b>Figure S6.</b> Effect of pH on the removal of TC: (a) adsorption and total removal	

efficiencies, (b) fitted rate constant  $k$ , (c) Zeta potentials of Cu/C-SiO<sub>2</sub> at different pH values and (d) the molecular formula for TC..... 14

**Figure S7.** Effect of HA on the removal of TC: (a) adsorption and total removal efficiencies, (b) fitted rate constant  $k$  (catalyst dosage = 1 g·L<sup>-1</sup>,  $C_0$  = 500 mg·L<sup>-1</sup>, pH = 3.65 ± 0.05, H<sub>2</sub>O<sub>2</sub> = 15 mL)..... 15

**Figure S8.** Different quenching scavengers in the Cu/C-SiO<sub>2</sub> + TC system: (a) adsorption and total removal efficiencies, (b) fitted rate constant  $k$  (catalyst dosage = 1 g·L<sup>-1</sup>,  $C_0$  = 500 mg·L<sup>-1</sup>, pH = 3.65 ± 0.05, H<sub>2</sub>O<sub>2</sub> = 15 mL)..... 16

**Figure S9.** Different concentrations of IPA in the Cu/C-SiO<sub>2</sub> + TC system: (a) adsorption and total removal efficiencies, (b) fitted rate constant  $k$  (catalyst dosage = 1 g·L<sup>-1</sup>,  $C_0$  = 500 mg·L<sup>-1</sup>, pH = 3.65 ± 0.05, H<sub>2</sub>O<sub>2</sub> = 15 mL)..... 17

**Figure S10.** Cyclic performance of Cu/C-SiO<sub>2</sub> + TC system: (a) adsorption and total removal efficiencies, (b) fitted rate constant  $k$  (catalyst dosage = 1 g·L<sup>-1</sup>,  $C_0$  = 500 mg·L<sup>-1</sup>, pH = 3.65 ± 0.05, H<sub>2</sub>O<sub>2</sub> = 15 mL). ..... 18

## Supporting information Texts

### Text S1. Characterization of the catalysts

The synthesized Cu/C-SiO<sub>2</sub> was characterized by transmission electron microscopy (TEM, JEOL 2100F) with an energy-dispersive X-ray spectrometer (EDS, Bruker XFlash 6T|60) elemental mapping. The mesoporous structure and phase components of the material were determined using an X-ray diffractometer (XRD, Bruker D8 Advance, Cu K $\alpha$  radiation, Germany). The N<sub>2</sub> adsorption-desorption isotherms were measured by a Micromeritics TriStar II 3020 system. The specific surface area and the pore size distribution of the material were calculated by the (BET) and Barrett-Joyner-Halenda (BJH) methods. Thermogravimetric (TG) analysis was conducted using a Perkin-Elmer instrument (SDT Q-600) with a heating rate of 20 °C min<sup>-1</sup> up to 800 °C under airflow. Surface groups and chemical states of the elements for the materials were examined by Fourier transform infrared (FTIR) spectra (Thermo Nicolet IS 10), and X-ray photoelectron spectroscopy (XPS, Thermo Fisher Scientific ESCALAB 250) measurements. Zeta potentials of the Cu/C-SiO<sub>2</sub> at different initial pH values were measured by Zeta-sizer Nano-ZS (Malvern ZEN3690). The TC concentration was determined by using a TU-1901 spectrophotometer at a maximum wavelength of around 357 nm.

**Text S2.** Analytical methods for adsorption and catalysis

The samples were taken by disposable syringe at different times and then filtrate was immediately collected through 0.45  $\mu\text{m}$  filter membrane to measure the absorbance.

The catalytic degradation curve was fitted by the first-order model (Eq. (1)):

$$-\ln(C_0/C_t) = kt \quad (1)$$

Among them,  $C_0$  and  $C_t$  are the initial concentration of TC and the concentration at time  $t$ ,  $\text{mg}\cdot\text{L}^{-1}$ ;  $k$  is the reaction rate coefficient,  $\text{min}^{-1}$ ;  $t$  is the reaction time, h.

## Supporting information Table

**Table S1.** N<sub>2</sub> adsorption/desorption results of the C-SiO<sub>2</sub> and Cu/C-SiO<sub>2</sub>.

Sample	$S_{\text{BET}}$ (m <sup>2</sup> ·g <sup>-1</sup> )	$V_{\text{P}}$ (cm <sup>3</sup> ·g <sup>-1</sup> )	$D_{\text{BJH}}$ (nm)
C/SiO <sub>2</sub>	756	1.01	10.78
Cu-C/SiO <sub>2</sub> (0.2)	509	0.65	9.94

$D_{\text{BJH}}$ : pore diameters were calculated from the adsorption branches.

**Table S2.** Reaction rate constants of TC degradation by CuO, Cu, C-SiO<sub>2</sub>, and Cu/C-SiO<sub>2</sub>.

Sample	reaction rate constant ( $k$ , min <sup>-1</sup> )
Cu-C/SiO <sub>2</sub>	0.05576
Cu	0.00957
CuO	0.00383
C/SiO <sub>2</sub>	0.00296

**Table S3.** The catalytic capacity of different catalyst towards TC.

catalyst	time (h)	$C_0$ ( $\text{mg}\cdot\text{L}^{-1}$ )	dose ( $\text{g}\cdot\text{L}^{-1}$ )	$C/C_0$ (%)	Reference
CuFeO <sub>2</sub> /BC	300	20	0.6	89.1	[1]
CuFeO <sub>2</sub> -NO/PBC	180	20	0.8	96.1	[2]
Cu/CuFe <sub>2</sub> O <sub>4</sub>	1120	50	0.3	75.4	[3]
SAS-Cu	30	20	0.1	82.5	[4]
Fe <sub>0.25</sub> Cu <sub>0.75</sub> (BDC)@DE	120	20	0.5	93.0	[5]
Cu/C-SiO <sub>2</sub>	240	500	1.0	99.9	This work

## Supporting information Figures

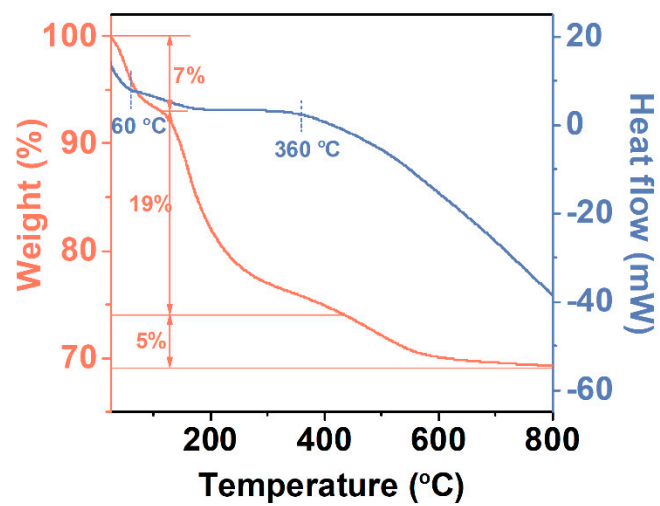


**Figure S1.** TG and DSC curves of the template-containing mesoporous SiO<sub>2</sub> sample.

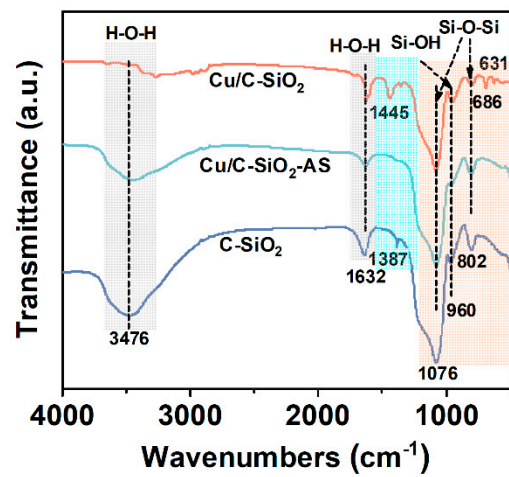


**Figure S2.** FTIR spectra of C-SiO<sub>2</sub>, Cu/C-SiO<sub>2</sub>-AS, and Cu/C-SiO<sub>2</sub>.

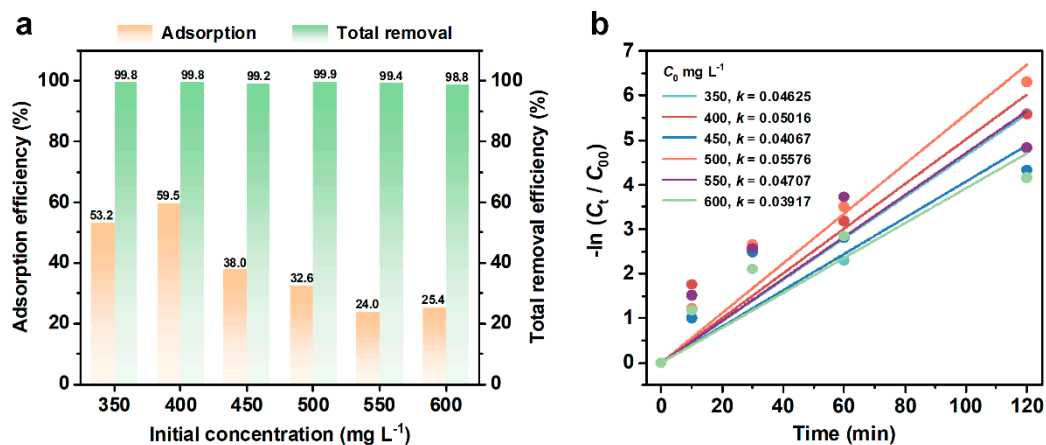


**Figure S3.** Effect of initial TC concentration on the removal of TC (catalyst dosage = 1 g·L<sup>-1</sup>, C<sub>0</sub> = 350–600 mg·L<sup>-1</sup>, H<sub>2</sub>O<sub>2</sub> = 15 mL, T = 20±2 °C): (a) adsorption and total removal efficiencies, (b) fitted rate constant *k*.

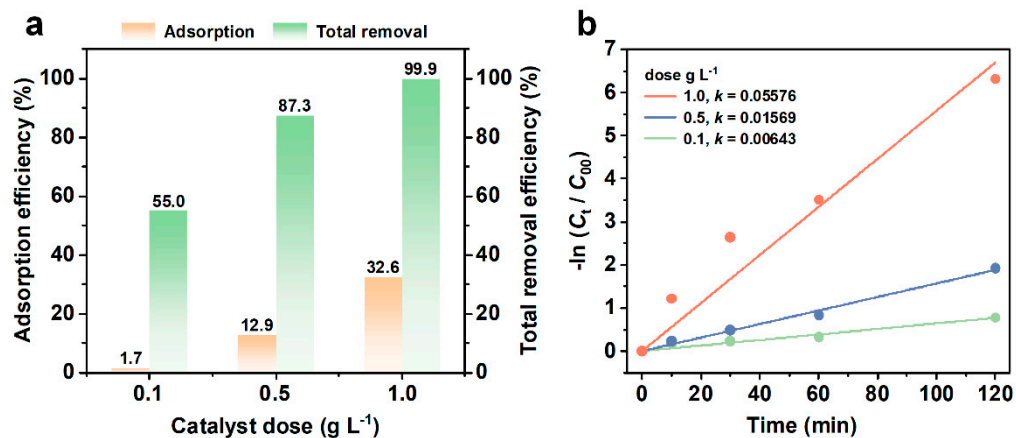


**Figure S4.** Effect of catalyst dosage on the removal of TC: (a) adsorption and total removal efficiencies, (b) fitted rate constant  $k$  ( $C_0 = 500 \text{ mg}\cdot\text{L}^{-1}$ ,  $\text{H}_2\text{O}_2 = 15 \text{ mL}$ ).

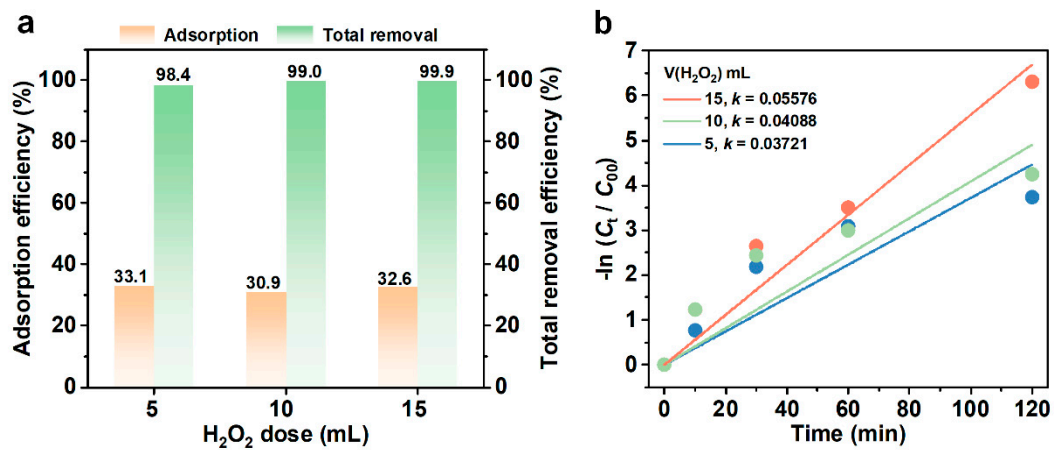


**Figure S5.** Effect of H<sub>2</sub>O<sub>2</sub> dosage on the removal of TC: (a) adsorption and total removal efficiencies, (b) fitted rate constant  $k$  (catalyst dosage = 1 g·L<sup>-1</sup>, C<sub>0</sub> = 500 mg·L<sup>-1</sup>)

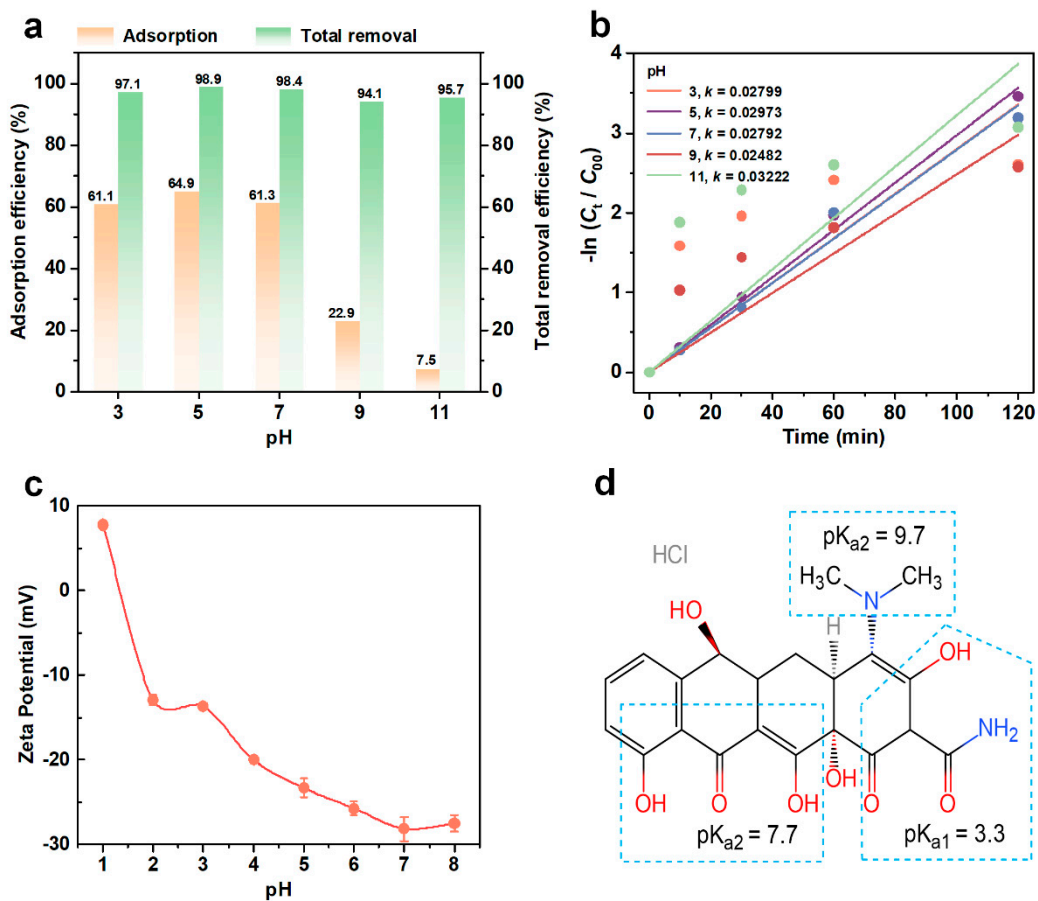


**Figure S6.** Effect of pH on the removal of TC: (a) adsorption and total removal efficiencies, (b) fitted rate constant  $k$ , (c) Zeta potentials of Cu/C-SiO<sub>2</sub> at different pH values and (d) the molecular formula for TC.

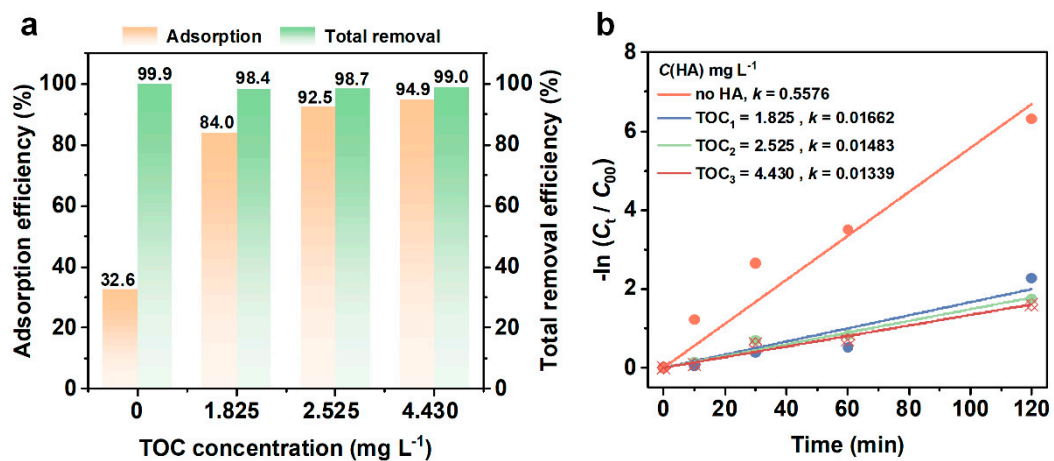


**Figure S7.** Effect of HA on the removal of TC: (a) adsorption and total removal efficiencies, (b) fitted rate constant  $k$  (catalyst dosage = 1 g·L<sup>-1</sup>, C<sub>0</sub> = 500 mg·L<sup>-1</sup>, pH = 3.65 ± 0.05, H<sub>2</sub>O<sub>2</sub> = 15 mL).

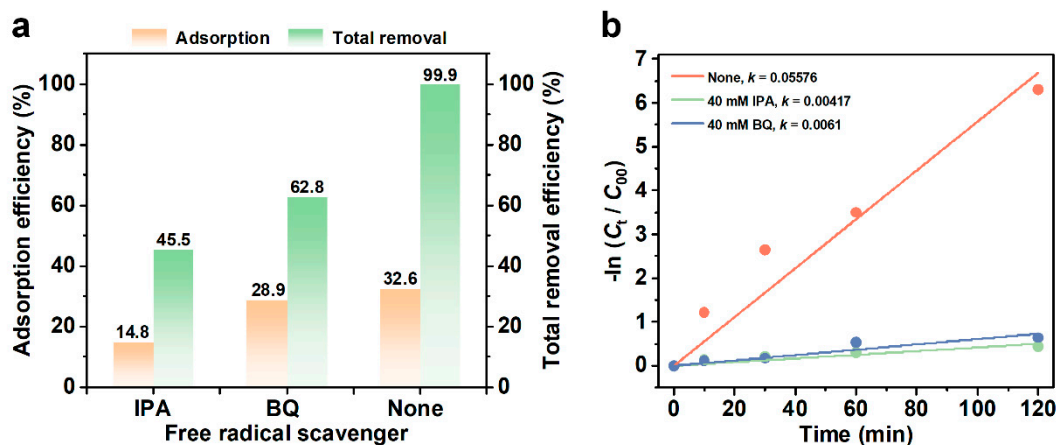


**Figure S8.** Different quenching scavengers in the Cu/C-SiO<sub>2</sub> + TC system: (a) adsorption and total removal efficiencies, (b) fitted rate constant  $k$  (catalyst dosage = 1 g·L<sup>-1</sup>, C<sub>0</sub> = 500 mg·L<sup>-1</sup>, pH = 3.65 ± 0.05, H<sub>2</sub>O<sub>2</sub> = 15 mL).

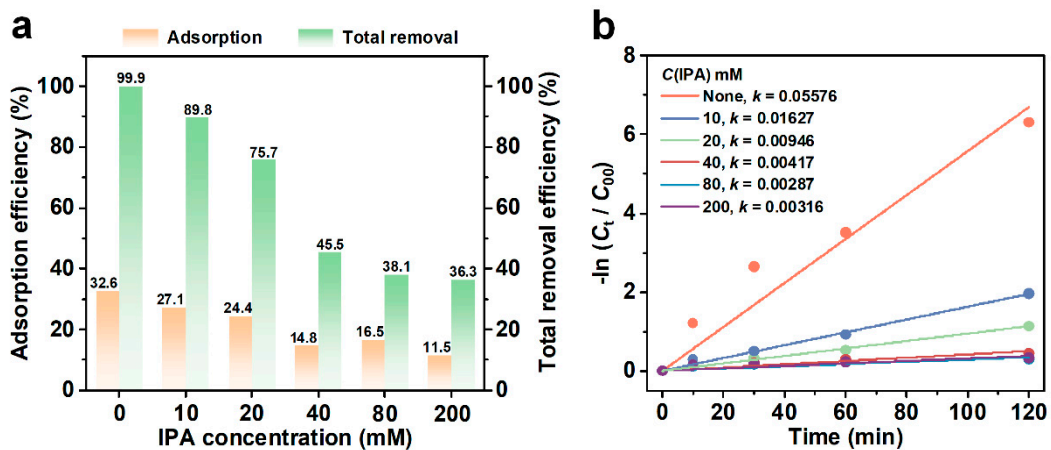


**Figure S9.** Different concentrations of IPA in the Cu/C-SiO<sub>2</sub> + TC system: (a) adsorption and total removal efficiencies, (b) fitted rate constant  $k$  (catalyst dosage = 1 g·L<sup>-1</sup>, C<sub>0</sub> = 500 mg·L<sup>-1</sup>, pH = 3.65 ± 0.05, H<sub>2</sub>O<sub>2</sub> = 15 mL).

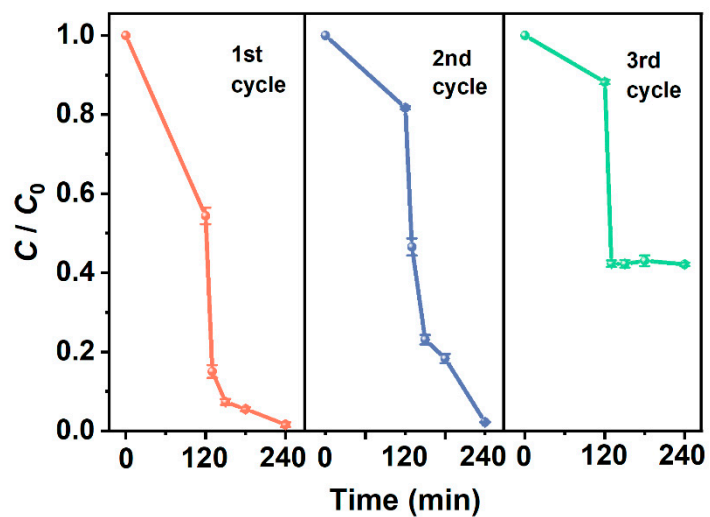


**Figure S10.** Cycling performance of Cu/C-SiO<sub>2</sub> (Adsorption for 2 hours, and catalytic reaction for 2 hours. Catalyst dosage = 1 g·L<sup>-1</sup>, C<sub>0</sub> = 500 mg·L<sup>-1</sup>, pH = 3.65 ± 0.05, H<sub>2</sub>O<sub>2</sub> = 15 mL).

## Reference

1. Xin, S.; Liu, G.; Ma, X.; Gong, J.; Ma, B.; Yan, Q.; Chen, Q.; Ma, D.; Zhang, G.; Gao, M.; et al. High efficiency heterogeneous Fenton-like catalyst biochar modified CuFeO<sub>2</sub> for the degradation of tetracycline: Economical synthesis, catalytic performance and mechanism. *Applied Catalysis B: Environmental* 2021, 280, 119386, doi:10.1016/j.apcatb.2020.119386.
2. Xin, S.; Huo, S.; Xin, Y.; Gao, M.; Wang, Y.; Liu, W.; Zhang, C.; Ma, X. Heterogeneous photo-electro-Fenton degradation of tetracycline through nitrogen/oxygen self-doped porous biochar supported CuFeO<sub>2</sub> multifunctional cathode catalyst under visible light. *Applied Catalysis B: Environmental* 2022, 312, 121442, doi:10.1016/j.apcatb.2022.121442.
3. Li, Z.; Guo, C.; Lyu, J.; Hu, Z.; Ge, M. Tetracycline degradation by persulfate activated with magnetic Cu/CuFe<sub>2</sub>O<sub>4</sub> composite: efficiency, stability, mechanism and degradation pathway. *Journal of Hazardous Materials* 2019, 373, 85-96, doi:10.1016/j.jhazmat.2019.03.075.
4. Liu, J.; He, H.; Shen, Z.; Wang, H.H.; Li, W. Photoassisted highly efficient activation of persulfate over a single-atom Cu catalyst for tetracycline degradation: Process and mechanism. *Journal of Hazardous Materials* 2022, 429, 128398, doi:10.1016/j.jhazmat.2022.128398.

5. Cui, K.P.; He, Y.Y.; Xu, K.J.; Zhang, Y.; Chen, C.B.; Xu, Z.J.; Chen, X.  
Degradation of tetracycline hydrochloride by Cu-doped MIL-101(Fe) loaded  
diatomite heterogeneous Fenton catalyst. *Nanomaterials* 2022, 12, 811,  
doi:10.3390/nano12050811.